LAWRENCE
LIVERMORE
NATIONAL
LABORATORY

LLNL-CONF-637437

Distinguishing Pu Metal from Pu Oxide Using Fast Neutron Counting

J. M. Verbeke, G. C. Chapline, L. F. Nakae, S. A. Sheets

May 24, 2013

Distinguishing Pu Metal from Pu Oxide Using Fast Neutron Counting
Palm Desert, CA, United States
July 14, 2013 through July 18, 2013

Disclaimer

DISTINGUISHING PU METAL FROM PU OXIDE USING FAST NEUTRON COUNTING

Jérôme M. Verbeke, George F. Chapline, Leslie F. Nakae, Steven A. Sheets
Lawrence Livermore National Laboratory
P.O. Box 808, Livermore, CA 94551

ABSTRACT

We describe a method for using fast neutron counting with scintillator detectors to simultaneously determining the α-ratio and the effective neutron multiplication factor k_{eff} for fissile materials using fast neutrons. Our method is a generalization of the Hage-Cifarelli method for determining k_{eff} for fissile assemblies which utilizes the shape of the fast neutron spectrum. In this talk we show that the fast neutron spectra generated by UO_2 and Pu metal samples and directly recorded in a liquid scintillator can be used to deduce the α-ratio of PuO_2 samples.

INTRODUCTION

Methods based on time-correlated neutron signals have long been used to characterize fissile materials. Typically one uses ^{3}He tubes to record the arrival times of neutrons from the fissile source, and then by segmenting the arrival times using time windows of varying width, one can use the statistics of the number of neutron counts in the time window as a function of the width of the time window to characterize the neutron source. Unfortunately the cross-section for neutron capture in ^{3}He is only large enough for the purposes of collecting these counting statistics after the fission neutrons have been thermalized in a moderating material. Therefore the time windows must be at least tens to hundreds of microseconds long in order to pick up the time correlation signals. In the case of a strong neutron source such as Pu this means that many fission chains will be generated within the time windows. Because the neutron time correlations of interest are generated by individual fission chains, the time correlation information that can be extracted using ^{3}He tubes is diluted.

Liquid scintillators on the other hand, can detect fission neutrons at their initial high energy, because the reaction used for detection is inelastic scattering of neutrons primarily on hydrogen, producing a recoil proton from which scintillation light is promptly produced. In contrast to ^{3}He tubes which can hardly detect any fast neutrons, liquid scintillators cannot detect any neutrons below 1 MeV, because the recoil proton for such neutrons do not produce enough scintillation light to distinguish them from the light produced by background gamma-ray interactions with the scintillator. At energies above 1 MeV, neutrons travel at a fraction of the speed of light, and can thus be detected within 100 nanoseconds for detections systems of the order of 1 meter in size. One no longer needs to open time windows as long as 100 μs to pick up the correlation signal with ^{3}He, but only as long as 100 ns. These shorter time windows will greatly reduce the number of overlapping chains within a time window and we will be in a regime where time windows encompass neutrons from single or mostly a few fission chains.

This report describes our efforts to use the time correlations of fast neutrons together with their energy spectra as measured directly in a liquid scintillator array to distinguish Pu metal from Pu oxide and also determine

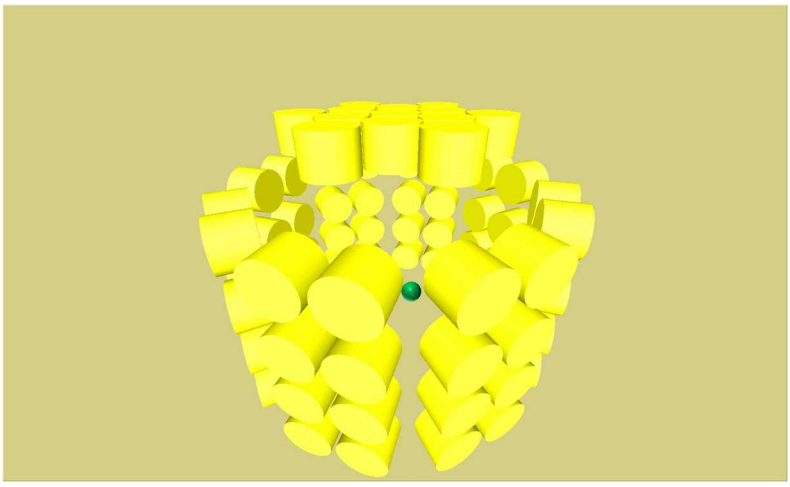

Figure 1: Object in the middle of the 77 liquid scintillator array.

the α-ratio of the Pu oxide. The liquid scintillator array used to obtain the results that we will discuss below is illustrated in Fig. 1. If the object at the center of the array contains a multiplying material, each spontaneous fission will typically generate a chain of detected neutrons in the liquid scintillator array. The fission chain will also generate gamma rays, but in the case of Pu the majority of the gamma rays are associated with Pu α-decay. An important difference between Pu metal and Pu oxide is that the α particles produced by the α-decay of Pu carry enough energy to cause ^{18}O to emit a neutron with an average energy of 1.9 MeV via an (α,n) reaction. These neutrons are emitted randomly, and in the case of Pu oxide the emission rate of these neutrons is comparable to the rate of neutron emission due to spontaneous fission. However, the energy spectra of the fission and (α,n) neutrons are different. We will show in the following that these differences can be exploited to determine the α-ratio, i.e. the ratio of the number of (α,n) neutrons to spontaneous fission neutrons.

DESCRIPTION OF PU OBJECTS MEASURED FOR THE REFERENCE NEUTRON SPECTRA

The algorithms developed in this paper rely upon the knowledge of two important neutron energy spectra: (a) the energy spectrum of fission neutrons, and (b) the energy spectrum of O(α,n) neutrons. If these two reference neutron energy spectra are sufficiently distinct, an arbitrary measured neutron energy spectrum should be reconstructable by combining the two reference spectra weighed appropriately.

To produce pure neutron spectra for both fission neutrons and O(α,n) neutrons, we need sources that will primarily produce these neutrons of interest.

Metallic plutonium

For objects containing only gram quantities of plutonium, the system does not multiply, and the neutron emission will be dominated by the spontaneous fission of ^{240}Pu. For kilogram quantities of metallic plutonium, the multiplication can be significant, i which case the fission neutron rate is dominated by induced fissions in ^{239}Pu. In general, the fission neutron energy spectrum will be a mix of ^{240}Pu spontaneous fissions and ^{239}Pu induced fissions. Fortunately, the fission neutron energy spectra for both ^{240}Pu and ^{239}Pu are very similar, as shown in Fig. 2. Therefore, the fission spectrum of objects containing plutonium will be insensitive to multiplication.

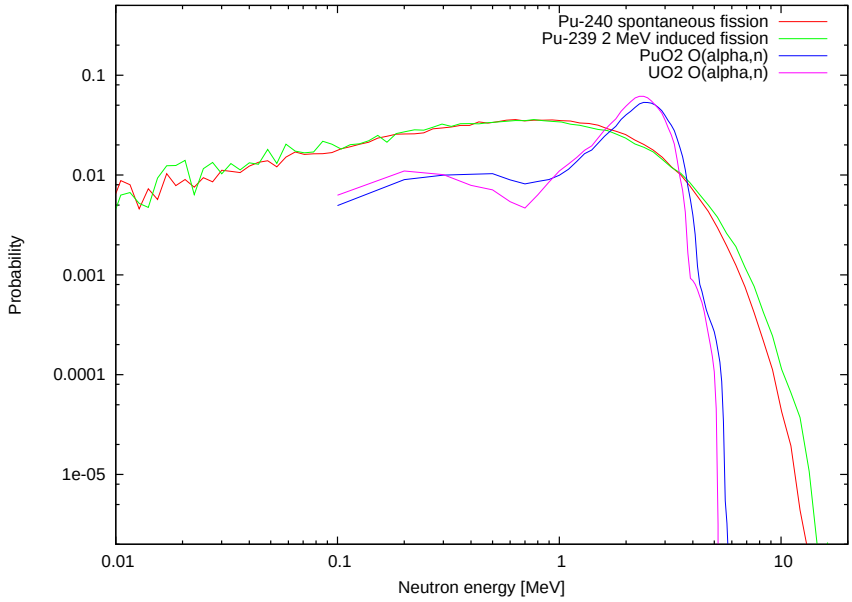

Figure 2: Energy distributions of neutrons from (a) ^{240}Pu spontaneous fission (red), (b) ^{239}Pu 2 MeV induced fission (green), O(α,n) reactions in (c) PuO_2 (blue) and (d) UO_2 (magenta). Fission spectra from Ref. [1], (α,n) spectra computed using SOURCE-4C [2].

In Fig. 3(b), we show the spectrum of energy deposited in our liquid scintillator by the fission neutrons for a bare 2.35 kg plutonium ball of density 15.92 g/cm^3 consisting of 93.88% ^{239}Pu, 5.96% ^{240}Pu, 0.13% ^{241}Pu, 0.37% ^{241}Am plus trace amounts of other isotopes.

Plutonium dioxide

For the oxide form of plutonium, namely PuO_2, the fast neutron spectrum will also contain a contribution from (α,n) neutrons. We have found from computer simulations that the ratio of the (α,n) neutron rate to the spontaneous fission neutron rate, also referred to as the α-ratio is of the order of 0.8. This α-ratio is a consequence of the fact that ^{240}Pu is a very strong spontaneous fission neutron source, and therefore in general the neutrons coming out of PuO_2 will contain comparable numbers of fission and \$$\alpha$,n) neutrons. If we were able to turn off fission reactions for both ^{239}Pu and ^{240}Pu, we could measure the O(α,n) neutron energy spectrum produced by the plutonium decay α-particles. While this would be possible in simulation, fission reactions cannot be turned off in nature. Of course, one might try using a theoretically derived (α,n) neutron spectrum to separate an observed fast neutron spectrum into a fission piece and an (α,n) piece. Unfortunately, converting a theoretical neutron spectrum into a liquid scintillator spectrum would require knowing how to convert an intrinsic neutron energy spectrum into a spectrum of liquid scintillator pulses with the pulse shape that one somewhat arbitrarily identifies as a neutron. This is very difficult to do in practice.

While we have a α-ratio of the order of 0.8 for PuO_2, the α-ratio is of the order of 30 or more for UO_2 (for an uranium composition close to HEU). This means that the vast majority of the neutrons emitted by uranium dioxide are O(α,n) neutrons. Measuring the spectrum of neutrons coming off of UO_2 would be roughly equiv-

alent to measuring the O(α,n) neutrons directly, without much pollution from fission neutrons. If it happened that the energy spectra of the O(α,n) neutrons from PuO_2 and UO_2 are similar, we could substitute PuO_2 with UO_2 to estimate the energy spectrum of PuO_2. Fig. 2 shows the energy distribution of O(α,n) neutrons (mainly from ^{18}O) for both PuO_2 (blue) and UO_2 (magenta). The (α,n) neutron spectra from PuO_2 and UO_2 are very close; therefore when analyzing the fast neutron spectrum from objects containing PuO_2 one can use the UO_2 (α,n) spectrum as a surrogate for the PuO_2 (α,n) spectrum. The objects used for measurement of the O(α,n) spectrum were 3 UO_2 objects of weights 1485.9, 1463.5, and 1516.7 g. The uranium in these objects consisted of 93.4% ^{235}U, 5.7% ^{238}U, 0.86% ^{234}U. The oxygen consisted in 99.8% ^{16}O, 0.04% ^{17}O and 0.2% ^{18}O. The total ^{18}O mass was 1 g, which is the source of the (α,n) neutrons.

The 3 uranium oxide objects were located in the middle of our array of liquid scintillators depicted in Fig. 1. The spectrum of energy deposited in the liquid scintillator by the UO_2 neutrons is shown in blue in Fig. 3(a). Because the UO_2 objects are weak neutron sources, we need to subtract the background that was present during the measurement to get to the UO_2 neutron spectrum. A 15-hour background spectrum was taken within 2 days of the experiment. The neutron energy spectrum from that background measurement is shown in green in Fig. 3(a). The rate of that background is 1.6 n/s and is likely due to cosmic-rays. Since the count rate for the measured objects is 13.52 n/s, the detection system system is measuring background neutrons 12% of the time. Thus, the blue curve in Fig. 3(a) contains both the UO_2 neutrons and 12% of background neutrons. Subtracting

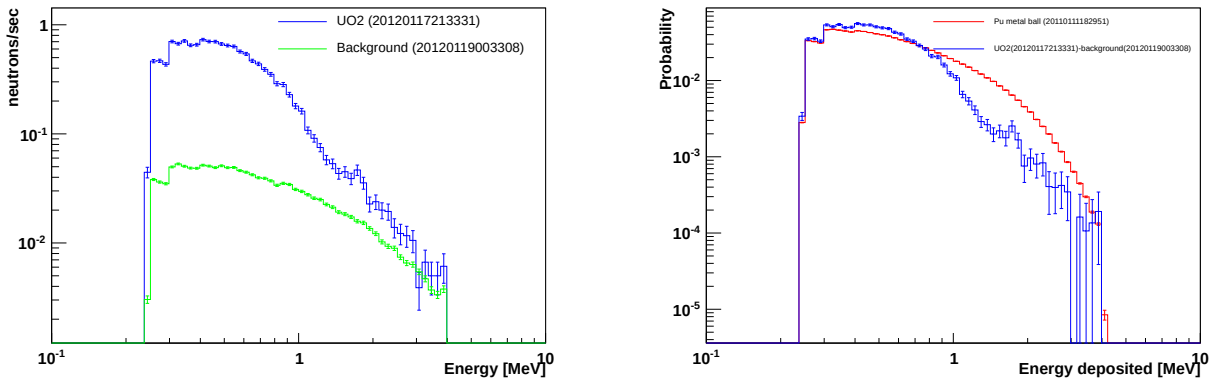

(a) Fast neutron rates versus energy for UO_2 objects (blue) and background (green).

(b) Fast neutron energy spectra for bare Pu metal ball (red) and UO_2 objects where the background was suppressed (blue).

Figure 3: Fast neutron energy spectra. The UO_2 curve represents 1800 s of data, the background 53,442 s, and the Pu metal ball 596 s. The measured count rates for the UO_2 objects, background and Pu metal were 13.52 n/s, 1.6 n/s, and 9123 n/s, respectively.

the background spectrum in green from the UO_2 spectrum in blue, we obtain the background-suppressed UO_2 neutron spectrum shown in blue in Fig. 3(b).

Regarding the fission neutrons emitted by both the spontaneous fissions of ^{238}U and the induced fissions in ^{235}U, since only 2 to 3% percents of the neutrons are due to fission in UO_2, the red curve in Fig. 3(b) would have to be shifted down by almost 2 orders of magnitude before being subtracted from the blue curve to produce a pure (α,n) neutron spectrum from uranium decay α-particles on oxygen. We can thus see that the normalized U fission curve would very small compared to the observed UO_2 curve, and therefore the effect of subtracting the U fission spectrum would be negligible. Given the resemblance between the (α,n) neutron energy spectra from UO_2 and PuO_2 (see Fig. 2), we will from this point on use the (α,n) neutron energy spectrum from UO_2 as a substitute for the (α,n) neutron energy spectrum for PuO_2.

MOMENT EQUATIONS WITH DIFFERENT MULTIPLICATIONS AND EFFICIENCIES FOR (α,n) NEUTRONS AND FISSION NEUTRONS

The times of arrival of the neutrons in each of the liquid scintillator cells were recorded. Randomly splitting the sequence of time tags into N segments of length T — where T is of the order of nanoseconds to hundreds of microseconds — one can count how many neutrons arrive in the first segment, how many in the second segment, in the third one, etc. and build distributions $b_n(T)$ of the number n of neutrons arriving in the segments of length T. For the sake of illustration, one such count distribution is shown in Fig. 4. By repeating this procedure for segments of different lengths T, multiple count distributions $b_n(T)$ can be obtained.

These count distributions $b_n(T)$ can be used to determine the strength F_s of the spontaneous fission sources in the object, the efficiency ε of the liquid scintillator array, and multiplication M of fissile material [3]. We will show these count distributions can also be used to determine the rate of neutrons from the (α,n) reactions. This will be shown by way of the first three moment equations for the count distributions. The first moment of the count distribution $b_n(T)$ is [5,6]

$$\bar{C}(T) = \left[\varepsilon_f q_f(M_f)\left[M_f + \alpha(M_\alpha - 1)\right]\bar{\nu}_s F_s + \varepsilon_\alpha q_\alpha(M_\alpha)\,\alpha\bar{\nu}_s F_s\right] T \tag{1}$$

where F_s is the strength of the spontaneous fission source in units of spontaneous fissions per second, α is the ratio of (α,n) neutrons to neutrons produced by spontaneous fission, ε_fq$_f$ and ε_αq$_\alpha$ are the detection efficiencies for fission and (α,n) neutrons, and M$_f$ and M$_\alpha$ are their neutron multiplications. $q(M)M$ is usually referred to as the escape multiplication and is given by

$$q(M)M = M - (M-1)/\bar{\nu} \tag{2}$$

The symbols $\bar{\nu}$ and $\bar{\nu}_s$ are the average numbers of neutrons emitted per induced and spontaneous fissions, respectively. They can be written as $\bar{\nu} = \sum_{n=1}^{8} nC_n$ and $\bar{\nu}_s = \sum_{n=1}^{8} nC_n^s$ where C_n and C_n^s are the probabilities of emitting n neutrons per induced and spontaneous fissions, respectively. The upper limit of 8 on the summation sign is the largest number of neutrons that known isotopes produce per fission. It should be noted that $\bar{\nu}$ depends on the energy of the neutron inducing fission.

We see in Fig. 2 that the energies of the neutrons from the reaction (α,n) on oxygen are typically higher than the fission neutron energies. Indeed, the mean fission neutron energy is about 1 MeV while the mean (α,n) neutron energy on oxygen is 2 MeV. This has two effects: (a) the average multiplicity $\bar{\nu}_\alpha$ due to (α,n) neutrons will be higher than the average multiplicity due to fission neutrons; (b) The detection efficiencies for (α,n) neutrons ε_α and fission neutrons ε_f will be different as well. Indeed for the case of PuO_2 the efficiency for detecting the oxygen (α,n) neutrons in our liquid scintillators will be significantly higher than for fission neutrons, because the energy spectrum for the (α,n) neutrons is peaked around 2 MeV where the intrinsic efficiency of the detector is relatively large, whereas almost half the fission neutrons have energies below 1 MeV where the intrinsic efficiency of our liquid scintillators is very small.

The slope of Eq. 1 is the average count rate

$$R_1 = \varepsilon_f q_f(M_f)\left[M_f + \alpha(M_\alpha - 1)\right]\bar{\nu}_s F_s + \varepsilon_\alpha q_\alpha(M_\alpha)\,\alpha\bar{\nu}_s F_s \tag{3}$$

The second and third moments of the $b_n(T)$ distribution, normalized by the count rate, are

$$Y_{2F}(T) = \frac{\left[\varepsilon_f q_f(M_f) M_f\right]^2}{\varepsilon_f q_f(M_f)\left[M_f + \alpha(M_\alpha - 1)\right] + \alpha\varepsilon_\alpha q_\alpha}\left[D_{2s} + \left[(M_f - 1) + \alpha(M_\alpha - 1)\right]D_2\right]\left(1 - \frac{1 - e^{-\lambda T}}{\lambda T}\right) \tag{4}$$

$$Y_{3F}(T) = \frac{\left[\varepsilon_f q_f (M_f) M_f\right]^3}{\varepsilon_f q_f (M_f)\left[M_f + \alpha(M_\alpha - 1)\right] + \alpha\varepsilon_\alpha q_\alpha}\left[D_{3s} + \left[(M_f - 1) + \alpha(M_\alpha - 1)\right] D_3\right]\left(1 - \frac{3 - 4e^{-\lambda T} + e^{-2\lambda T}}{2\lambda T}\right)$$
$$+ 2\frac{\left[\varepsilon_f q_f (M_f) M_f\right]^3}{\varepsilon_f q_f (M_f)\left[M_f + \alpha(M_\alpha - 1)\right] + \alpha\varepsilon_\alpha q_\alpha}(M_f - 1)\left[D_{2s}D_2 + \left[(M_f - 1) + \alpha(M_\alpha - 1)\right] D_2^2\right]\left(1 - \frac{2 - (2 + \lambda T)e^{-\lambda T}}{\lambda T}\right) \quad (5)$$

where λ is a time constant related to the transport of the neutrons in the measured object and the detection system, the parameters D_{2s}, D_2, D_{3s} and D_3 depend on nuclear data, and are given by $D_{2s} = \frac{\sum_{n=2}^{8}\binom{n}{2}C_n^s}{\bar{\nu}_s}$ and $D_2 = \frac{\sum_{n=2}^{8}\binom{n}{2}C_n}{\bar{\nu}}$, $D_{3s} = \frac{\sum_{n=3}^{8}\binom{n}{3}C_n^s}{\bar{\nu}_s}$ and $D_3 = \frac{\sum_{n=3}^{8}\binom{n}{3}C_n}{\bar{\nu}}$.

The fission cross-sections for fission and (α,n) neutrons are nearly the same for all the energies of interest. Therefore, if we neglect the small difference between $\bar{\nu}_\alpha$ and $\bar{\nu}$, we can set $M_\alpha = M_f \equiv M$. The system of equations 3 through 5 now has 5 unknown parameters: M, $\varepsilon_f q_f$, $\varepsilon_\alpha q_\alpha$, α, F_s. Defining R_{2F} and R_{3F} as the asymptotical values of $Y_{2F}(T)$ and $Y_{3F}(T)$, and following Cifarelli-Hage, we can contemplate writing the ratio R_{3F}/R_{2F}^2 to determine the multiplication M:

$$\frac{R_{3F}}{R_{2F}^2} = \frac{2(M-1)D_2\left[D_{2s} + (1+\alpha)(M-1)D_2\right] + D_{3s} + (1+\alpha)(M-1)D_3}{\left[D_{2s} + (1+\alpha)(M-1)D_2\right]^2}\left(\frac{R_1}{\varepsilon_f q M \bar{\nu}_s F_s}\right) \quad (6)$$

Unfortunately, we cannot use expression 6 directly to determine the multiplication because of the presence of too many unknown parameters: M, α, ε_f, and ε_α.

We can replace the two efficiencies by a single parameter by making use of the theoretical fission and (α,n) spectra shown in Fig. 2 to calculate the ratio $\varepsilon_\alpha/\varepsilon_f$. Calling this ratio r_ε we have

$$\frac{R_{3F}}{R_{2F}^2} = \frac{2(M-1)D_2\left[D_{2s} + (1+\alpha)(M-1)D_2\right] + D_{3s} + (1+\alpha)(M-1)D_3}{\left[D_{2s} + (1+\alpha)(M-1)D_2\right]^2}\left[\left[1 + \alpha\left(\frac{M-1}{M}\right)\right] + r_\varepsilon\frac{\alpha}{M}\right] \quad (7)$$

The efficiency ratio r_ε depends on the theoretical fission and (α,n) neutron spectra and the characteristics of the neutron detector. For our liquid scintillators we find $r_\varepsilon \sim 1.602$. Given a value for r_ε one can in principle use Eq. 7 to solve for the multiplication as a function of α. Unfortunately this equation is now a cubic equation rather than the quadratic equation in the $\alpha = 0$ case considered by Cifarelli and Hage.

As an alternative we can use the observed liquid scintillator spectrum to directly evaluate the quantity $\left[1 + \alpha\left(\frac{M-1}{M}\right)\right] + r_\varepsilon\frac{\alpha}{M}$ in Eq. 7. In particular, if we neglect the background contribution, fitting the observed fast neutron spectrum to a sum of fission and (α,n) spectra yields two coefficients whose ratio ρ should be equal to $\frac{r_\varepsilon\alpha}{M+\alpha(M-1)}$. Given this additional experimental input, one can rewrite Eq. 7 as

$$\frac{R_{3F}}{R_{2F}^2} = \frac{2(M-1)D_2\left[D_{2s} + (1+\alpha)(M-1)D_2\right] + D_{3s} + (1+\alpha)(M-1)D_3}{\left[D_{2s} + (1+\alpha)(M-1)D_2\right]^2}\left[1 + \alpha\left(\frac{M-1}{M}\right)\right](1+\rho) \quad (8)$$

Using the definition of ρ, we can write the following relationship between α and M:

$$\alpha = \frac{M}{\frac{r_\varepsilon}{\rho} - M + 1} \quad (9)$$

In the limit of small ρ, $\alpha \to \frac{\rho}{r_\varepsilon}$, while in the limit of large α, $\rho \to \frac{r_\varepsilon}{M-1}$ so it becomes very difficult to determine the α-ratio from the spectral shape when α is large. Substituting Eq. 9 into 8, we find that α becomes the

solution of the following quadratic equation:

$$2D_2\left(\frac{\alpha r_\varepsilon}{\rho}-1\right)\left[D_{2s}+\left(\frac{\alpha r_\varepsilon}{\rho}-1\right)D_2\right]+(1+\alpha)\left[D_{3s}+\left(\frac{\alpha r_\varepsilon}{\rho}-1\right)D_3\right]=\frac{1+\frac{\rho}{r_\varepsilon}}{1+\rho}\frac{R_{3F}}{R_{2F}^2}\left[D_{2s}+\left(\frac{\alpha r_\varepsilon}{\rho}-1\right)D_2\right]^2 \quad (10)$$

In the next sections, we show that this equation together with the spectral information in the liquid scintillators can be used to solve for the α ratio and the multiplication.

LIQUID SCINTILLATOR TIME CORRELATION RESULTS

For the 2.35 kg Pu ball previously described, the count distribution for T=1 μs, and the moments $Y_{2F}(T)$ and $Y_{3F}(T)$ are shown in Fig. 4. The total time is shared among the 6 time gates in such a way as to keep the errors on the $Y_{2F}(T)$ and $Y_{3F}(T)$ values for the different time gates approximately equal. Fast neutron counts are not re-used among different time gates. These data correspond to a measurement of 113 seconds, 21.2 seconds of which contributed to the 1 μs time gate, and the remaining time was shared among the other time gates. The values of R_1, R_{2F} and R_{3F} can be extracted from the graphs.

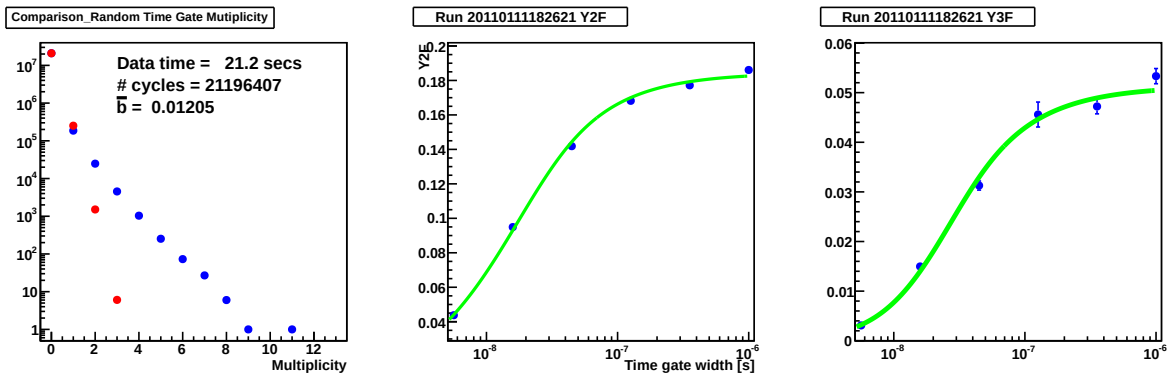

Figure 4: Count distribution $b_n(T)$ for the 1 μs time gate, $Y_{2F}(T)$ and $Y_{3F}(T)$ for the Pu ball and T between 5 ns and 1 μs, along with their theoretical reconstructions in green. The set of parameters used for the moment reconstruction (M,ε_f,α)=(2.1, 4.6%, 0.006) was determined using the measured moments and the spectral information.

Fig. 5 shows the results for a PuO_2 sample containing 8.72 g of plutonium. The measurement thereof was much longer as the weight of PuO_2 was just a few grams.

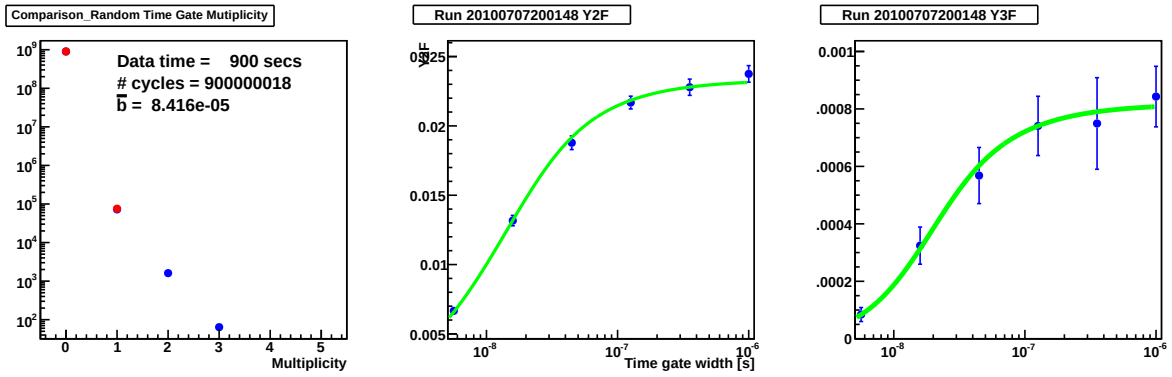

Figure 5: Count distribution $b_n(T)$ for the 1 μs time gate, $\bar{C}(T)$, $Y_{2F}(T)$ and $Y_{3F}(T)$ for the PuO_2 sample and T between 5 ns and 1 μs, along with their theoretical reconstructions in green. The set of parameters used for the moment reconstruction (M,ε_f,α)=(1.06, 5.1%, 0.86) was determined using the measured moments and the spectral information.

LIQUID SCINTILLATORS SPECTRAL INFORMATION

In this section we describe experimental results which illustrate how the information contained in the spectrum of energies deposited by the fast neutrons in the liquid scintillator cells can be used to differentiate metallic plutonium from plutonium dioxide. For the measured PuO_2 sample, the spectrum of energies deposited by the fast neutrons is shown in green in Fig 6, along with the Pu metal neutron spectrum in red and the pure (α,n) neutron spectrum from α-particles on oxygen in blue (the latter two directly copied from Fig. 3(b)). In Fig. 7 we show that the red and blue spectra can be added with suitable weights to reconstruct the green curve. In particular, by adding the ^{240}Pu spectrum pre-multiplied by 0.45 to the (α,n) spectrum pre-multiplied by 0.55, one obtains the reconstruction spectrum of energies deposited shown in red in Fig. 7(b). On the other hand, when one measures the Pu metal ball, the weights that are optimal for the reconstruction of the spectrum of deposited energies are 0.995 of the ^{240}Pu spectrum and 0.005 of the (α,n) spectrum. So we find that just measuring the spectrum of energies deposited in a liquid scintillator by fast neutrons is sufficient to distinguish Pu metal and Pu oxide.

Setting ρ=1.24, the solution to Eqs. 9-10 with $M \geq 1$ is $\alpha = 0.86 \pm 0.08$, $M = 1.06 \pm 0.09$. The exact value of 0.8 for α is within 1 standard deviation of our solution. Using Eq. 4, we determined the value of ε_f to be 5.1%, while Eq. 1 implies a spontaneous fission source rate of 662 ± 57 neutrons/sec. Although not exactly the same strength as the true value of 519 n/s, the implied spontaneous fission rate is within 20% of the correct answer. If we measure 10 times longer, the solution with $M \geq 1$ becomes $\alpha = 0.84 \pm 0.02$, $M = 1.05 \pm 0.02$, ε_f=5.3%, and the spontaneous fission source rate becomes 638 ± 11 neutrons/sec. For the metallic plutonium ball, our algorithm gives ρ=0.005. The solution to Eqs. 9-10 with $M \geq 1$ is $\alpha = 0.006 \pm 0.0001$, $M = 2.1 \pm 0.04$. The value of ε_f is 4.6% and the source strength is $149,015 \pm 2,700$ neutrons/sec, which is off the true value by less than 1.5%, or less than 1 standard deviation.

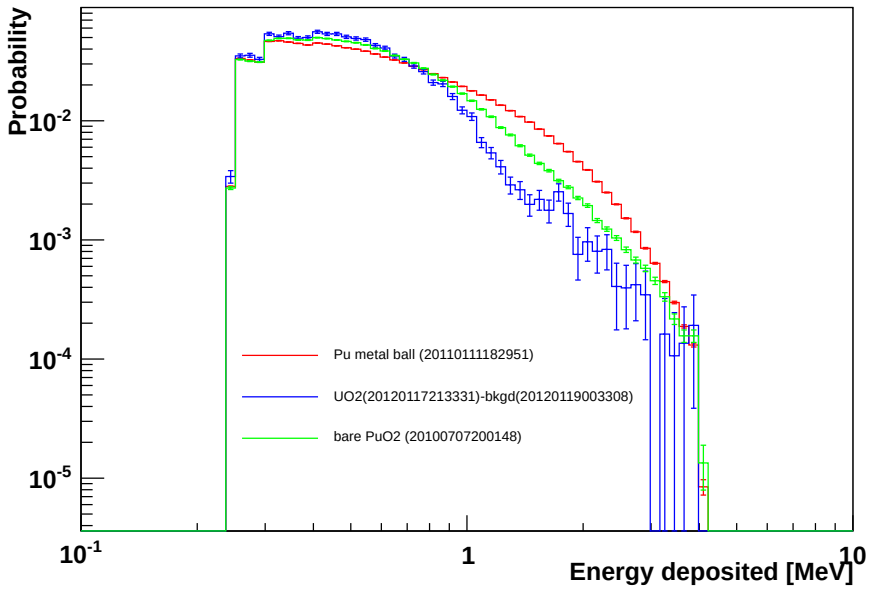

Figure 6: Fast neutron energy spectra for PuO_2 sample (green), along with Pu metal ball (red) and modified UO_2 (blue) spectra. The experimental curve for PuO_2 represents 7200 s of data.

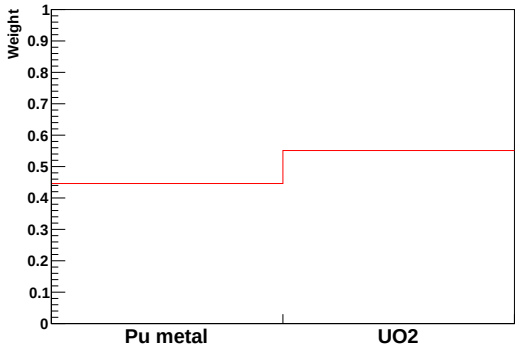

(a) Factors by which the blue and red spectra shown in Fig. 6 must be multiplied to reconstruct the spectrum of energies deposited by the fast neutrons emitted by the PuO_2 sample: 0.45 for the Pu metal spectrum and 0.55 for the UO_2 sample spectrum.

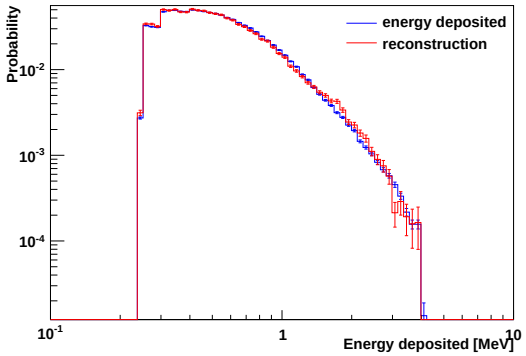

(b) Spectrum of energies deposited by fast neutrons in liquid scintillator cells for the PuO_2 sample (blue), along with its reconstruction (red) from the blue and red spectra shown in Fig. 6 and the optimal weights shown on the left.

Figure 7: Reconstruction of the PuO_2 objects using the sum of two weighed energy spectra.

CONCLUSION

In this paper, we have shown first of all that measuring the energy spectrum of the fast neutrons using a liquid scintillator allows one to distinguish the metallic and oxide forms of plutonium. In addition, combining this information with the Feynman 2-neutron and 3-neutron correlations allows one to extract the α-ratio without explicitly knowing the multiplication. Given the α-ratio one can then extract the multiplication as well as the ^{239}Pu and ^{240}Pu masses directly from the moment equations. In principle the same techniques could be used to

distinguish metallic Pu from other compounds of Pu, such as PuF_2, where (α,n) neutron emission is significant.

ACKNOWLEDGMENTS

This work performed under the auspices of the U.S. Department of Energy by Lawrence Livermore National Laboratory under Contract DE-AC52-07NA27344.

References

[1] J.M. Verbeke, C. Hagmann, D. Wright, "Simulation of Neutron and Gamma Ray Emission from Fission and Photofission," LLNL-AR-228518, Lawrence Livermore National Laboratory (2010). 3

[2] W.B. Wilson, R.T. Perry, E.F. Shores, W.S. Charlton, T.A. Parish, G.P. Estes, T.H. Brown, E.D. Arthur, M. Bozoian, T.R. England, D.G. Madland, and J.E. Stewart, "SOURCES 4C: A Code for Calculating (alpha,n), Spontaneous Fission, and Delayed Neutron Sources and Spectra," LA-UR-02-1839, Los Alamos National Laboratory (2002). 3

[3] M.K. Prasad, N.J. Snyderman, "Statistical Theory of Fission Chains and Generalized Poisson Neutron Counting Distributions," *Nucl. Sci. and Eng.* **172**, 300-326 (2012). 5

[4] J.M. Verbeke, G.F. Chapline, "Distinguishing Plutonium Metal From Plutonium Oxide," LLNL-TR-518451, Lawrence Livermore National Laboratory (2011).

[5] W. Hage, D.M. Cifarelli, "Correlation Analysis with Neutron Count Distributions in Randomly or Signal Triggered Time Intervals for Assay of Special Fissile Materials," *Nucl. Sci. and Eng.* **89**, 159-176 (1985). 5

[6] D.M. Cifarelli, W. Hage, "Models for a Three-Parameter Analysis of Neutron Signal Correlation Measurements for Fissile Material Assay," *Nucl. Instr. and Meth. in Phys. Res.* **A251**, 550-563 (1986). 5